Inorg. Chem. **2005**, *44*, 911–920

Systematic Investigation of the Hydrothermal Syntheses of Pr(III)–PDA (PDA = Pyridine-2,6-dicarboxylate Anion) Metal–Organic Frameworks

Bin Zhao, Long Yi, Yan Dai, Xiao-Yan Chen, Peng Cheng,* Dai-Zheng Liao, Shi-Ping Yan, and Zong-Hui Jiang

Department of Chemistry, Nankai University, Tianjin 300071 (China)

Received April 17, 2004

A series of novel two-dimensional (2D) and three-dimensional (3D) praseodymium coordination polymers, namely, $\{[Pr_3(PDA)_4(HPDA)(H_2O)_8]\cdot 8H_2O\}_n$ (**2**), $\{[Pr_2(PDA)_3(H_2O)_3]\cdot H_2O\}_n$ (**3**), $\{[Pr(PDA)(H_2O)_4]\cdot ClO_4\}_n$ (**4**), and $\{[Pr_2(PDA)_2(H_2O)_5SO_4]\cdot 2H_2O\}_n$ (**5**) (PDA = pyridine-2,6-dicarboxylic anion), was designed and synthesized under hydrothermal conditions. Complexes **1**–**3** (chainlike polymer, $\{[Pr(PDA)(HPDA)(H_2O)_2]\cdot 4H_2O\}_n$ (**1**) was also obtained independently by us, although it has been reported recently by Ghosh et al.) were fabricated successfully by simply tuning the Pr/PDA ratio and exhibited various and intriguing topological structures from a 1D chain to a 3D network. While the synthetic strategy of **5** was triggered and further performed only after **1** was structurally characterized**.** The complexes were characterized by X-ray single-crystal determination, spectroscopic, and variable-temperature magnetic susceptibility analyses. In complex **2** an unusual nanosized square motif as a building block constructed by eight Pr ions was further assembled into a highly ordered 2D grid compound. In complex **3** the decanuclear Pr metal-based structure as a repeat unit interpenetrated to form a novel 3D polymer. Complex **4** was a 3D network polymer fabricated through a hexanuclear Pr ring as a building block, and ClO_4^- anions as guests were trapped in the cavity. In complex **5** six Pr atoms, two SO_4^{2-} anions, and carboxylic oxygen bridges constructed an intriguing rectangle structure as a repeat unit in the grid to form a 2D coordination polymer in which the unique bi-bidentate coordination mode of SO_4^{2-} anion was observed.

Introduction

The fabrication of multidimensional arrays and networks comprised of metal ions as nodes and bridged ligands as spacers of self-assembly has made great progress in the past decade or so.[1,2] Chemists are attracted by the beautiful and intriguing topological structures which can be obtained by assembling metal ions and multifunctional ligands. Thus, many spectacular polymers have been documented, such as 1D chains[3] and ladders,[4] 2D grids,[5] 3D porous motifs, interpenetrated mode, and helical staircase networks.[6] In particular, a large number of grid networks containing cavities with diverse sizes and shapes were formed predominantly due to introduction of the 3d-block metal ions.[7] However, to the best of our knowledge, examples of lanthanide-based 2D grids and 3D networks are relatively scarce.[8]

* To whom correspondence should be addressed. E-mail: pcheng@nankai.edu.cn.

(1) (a) Whitesides, G. M.; Grzybowski, B. *Science* **2002**, *295*, 2418. (b) Fujita, M.; Kwon, Y. J.; Washizu, S.; Ogura, K. *J. Am. Chem. Soc.* **1994**, *116*, 1151. (c) Janiak, C. *Dalton Trans.* **2003**, 2781. (d) Moulton, B.; Zaworotko, M. J. *Chem. Rev.* **2001**, *101*, 1629.

(2) For example: (a) Kepert, C. J.; Rosseinsky, M. J. *Chem. Commun.* **1999**, 375. (b) Eddaoudi, M.; Moler, D. B.; Li, H.; Chen, B.; Reinecke, T. M.; O'Keeffe, M.; Yaghi, O. M. *Acc. Chem. Res.* **2001**, *34*, 319.

(3) (a) Shin, D. M.; Lee, I. S.; Lee, Y. A.; Chung, Y. K. *Inorg. Chem.* **2003**, *42*, 2977. (b) Withersby, M. A.; Blake, A. J.; Champness, N. R.; Hubberstey, P.; Li, W. S.; Schröder, M. *Angew. Chem., Int. Ed. Engl.* **1997**, *39*, 22327. (c) Batsanov, A. S.; Begley, M. J.; Hubberstey, P.; Stroud, J. *J. Chem. Soc., Dalton Trans.* **1996**, 1947.

(4) (a) Withersby, M. A.; Blake, A. J.; Champness, N. R.; Cooke, P. A.; Hubberstey, P.; Li, W. S.; Schröder, M. *Inorg. Chem.* **1999**, *38*, 2259. (b) Nomiya, K.; Yokoyama, H. *J. Chem. Soc., Dalton Trans.* **2002**, 2483.

(5) (a) Shin, D. M.; Lee, I. S.; Chung, Y. K.; Lah, M. S. *Inorg. Chem.* **2003**, *42*, 5459. (b) Mitsurs, K.; Shimamura, M.; Noro, S. I.; Minakoshi, S.; Asami, A.; Seki, K.; Kitagawa, S. *Chem. Mater.* **2000**, *12*, 1288. (c) Carlucci, L.; Ciani, G.; Proserpio, D. M. *J. Chem. Soc., Dalton Trans.* **1999**, 1799. (d) He, C.; Zhang, B. G.; Duan, C. Y.; Li, J. H.; Meng, Q. J. *Eur. J. Inorg. Chem.* **2000**, 2549.

(6) (a) Eddaoudi, M.; Kim, J.; Rosi, N.; Vodak, D.; Wachter, J.; O'Keeffe, M.; Yaghi, O. M. *Science* **2002**, *295*, 469. (b) Wu, C. D.; Lu, C. Z.; Zhuang, H. H.; Huang, J. S. *J. Am. Chem. Soc.* **2002**, *124*, 3836. (c) Wang, R.; Gao, E.; Hong, M.; Gao, S.; Luo, J.; Lin, Z. *Inorg. Chem.* **2003**, *42*, 5486. (d) Reineke, T. M.; Eddaoudi, M.; Moler, D.; O'Keeffe, M.; Yaghi, O. M. *J. Am. Chem. Soc.* **2000**, *122*, 4843. (e) Reineke, T. M.; Eddaoudi, M.; Moler, D.; O'Keeffe, M.; Yaghi, O. M. *J. Am. Chem. Soc.* **2000**, *122*, 4843. (f) Stuart, R. B.; Richard, R. *Angew. Chem., Int. Ed.* **1998**, *37*, 1460.

(7) (a) Vilminot, S.; Richard-Plouet, M.; André, G.; Swierczynski, D.; Bourée-Vigneron, F.; Kurmoo, M. *Inorg. Chem.* **2003**, *42*, 6859. (b) Wickleder, M. S. *Z. Anorg. Allg. Chem.* **2001**, *627*, 2112.

10.1021/ic049498m CCC: $30.25
Published on Web 01/19/2005

On the other hand, incorporation of trivalent lanthanide ions into the self-assembling molecular architecture is currently of great interest in view of their interesting magnetic and luminescent properties[9] as well as great potential applications,[10−12] for example, catalysis, adsorption, separation, sensor, and molecular recognition. Indeed, fabrication of multidimensional coordination polymers by the self-assembly process is crucial for the design of lanthanide-based devices such as light converters.[13] However, the variable and high coordination numbers of the trivalent lanthanide ions and the small energy difference between the various coordination geometries showing low stereochemical preference make rational design for the self-assembly of lanthanide complexes quite challenging.[14−16] Therefore, multidimensional coordination polymers comprised of 4f-metal ions and associated with the self-assembly processes remain relatively unexplored so far.[17,18] At the same time, to date, no systematic investigation on the relationship between the self-assembly of lanthanide-based complexes and different Ln/L ratio has been carried out.[19,20]

In addition, selection of the polydentate organic ligand is a key point to design and assemble expected polymers. In our studies a simple and suitable polydentate ligand H_2PDA (pyridine-2,6-dicarboxylic acid) was employed. H_2PDA has a rigid 120° angle between the central pyridine ring and the two carboxylic acid groups and therefore could potentially provide both discrete and consecutive metal complexes under appropriate conditions. Though many complexes of this ligand containing trivalent or tetravalent lanthanide ions have been reported, the Ln/L ratio of these lanthanide complexes is always 1/3.[21−24]

In this contribution, using the tridentate ligand PDA, we successfully isolated five coordination polymers based on praseodymium ion $\{[Pr(PDA)(HPDA)(H_2O)_2]\cdot 4H_2O\}_n$ (**1**),[25] $\{[Pr_3(PDA)_4(HPDA)(H_2O)_8]\cdot 8H_2O\}_n$ (**2**), $\{[Pr_2(PDA)_3(H_2O)_3]\cdot H_2O\}_n$ (**3**), $\{[Pr(PDA)(H_2O)_4]\cdot ClO_4\}_n$ (**4**), and $\{[Pr_2(PDA)_2(H_2O)_5SO_4]\cdot 2H_2O\}_n$ (**5**) by reaction of Pr_6O_{11} with H_2PDA ligand under hydrothermal conditions. Complexes **1**−**3** were fabricated successfully by simply tuning different Pr/PDA ratios under the same synthetic conditions, while the synthetic strategy of **5** was triggered and further performed only after **1** was structurally characterized**.** These complexes were characterized by X-ray crystal determination, spectroscopic, and variable-temperature magnetic susceptibility analyses. The striking feature of **2**−**5** is that these complexes exhibit beautiful topological structures: **2** has an octanuclear homometallic Pr_8 square structure as a construction unit to form a 2D grid; **3** is a 3D polymer interpenetrated via decanuclear metal-based units, while **4** possesses a hexanuclear Pr ring as a building block to form a 3D network polymer. **5** contains a hexanuclear homometallic Pr_6 square unit to form a 2D coordination polymer in which the unprecedented bi-bidentate coordination mode of the SO_4^{2-} anion is observed for the first time.

Experimental Section

Materials and Physical Techniques. All reagents and solvents employed were commercially available and used as received without further purification. Analyses for C, H, and N were carried out on a Perkin-Elmer analyzer at the Institute of Elemento-Organic Chemistry, Nankai University. Infrared spectra were measured on a Bruker Vector 22 FT-IR instrument from KBr pellets. Variable-temperature magnetic susceptibilities were measured on a Quantum Design MPMS-7 SQUID magnetometer. Diamagnetic corrections were made with Pascal's constants for all the constituent atoms. Powder X-ray diffraction measurements were recorded on a D/Max-2500 X-ray diffractometer using Cu Kα radiation. Thermal analyses (under oxygenated atmosphere, heating rate of 5 °C/min) were carried out in a Labsys NETZSCH TG 209 Setaram apparatus.

Preparations. $\{[Pr(PDA)(HPDA)(H_2O)_2]\cdot 4H_2O\}_n$ **(1).** The synthesis of **1** is described in the Supporting Information.

$\{[Pr_3(PDA)_4(HPDA)(H_2O)_8]\cdot 8H_2O\}_n$ **(2).** A mixture of pyridine-2,6-dicarboxylic acid (1.0 mmol, 0.167 g), Pr_6O_{11} (0.1 mmol, 0.102 g), H_2O (10 mL), and C_2H_5OH (2 mL) was placed in a 25 mL acid-digestion bomb at 180 °C for 3 days. The products (0.138

(8) (a) Zaworotko, M. J. *Chem. Commun.* **2001**, 1. (b) Reineke, T. M.; Eddaoudi, M.; Moler, D.; O'Keeffe, M.; Yaghi, O. M. *J. Am. Chem. Soc.* **2000**, *122*, 4843. (c) Goodgame, D. M. L.; Hill, S. P. W.; Williams, D. J. *Inorg. Chim. Acta* **1998**, *272* (1, 2), 131.

(9) (a) Benelli, C.; Gatteschi, D. *Chem. Rev.* **2002**, *102*, 2369. (b) Piguet, C.; Bernardinelli, G.; Hopfgartner, G. *Chem. Rev.* **1997**, *97*, 2005. (c) Bernardinelli, G.; Hopfgartner, G.; Petoud, S.; Schaad, O. *J. Am. Chem. Soc.* **1996**, *118*, 6681. (d) Sabbatini, N.; Guardigli, M.; Lehn, J. M. *Coord. Chem. Rev.* **1993**, *123*, 201. (e) Kido, J.; Okamoto, Y. *Chem. Rev.* **2002**, *102*, 2357. (f) Zhao, H.; Bazile, M. J.; Galán-Mascarós, J. R.; Dunbar, K. R. *Angew. Chem., Int. Ed.* **2003**, *42*, 1015. (g) Reinhard, C.; Gudel, H. U. *Inorg. Chem.* **2002**, *41*, 1048.

(10) (a) Zaworotko, M. J. *Chem. Soc. Rev.* **1994**, 283. (b) Batten, S. R.; Robson, R. *Angew. Chem., Int. Ed.* **1998**, *37*, 1460. (c) Gardner, G. B.; Venkataraman, D.; Moore, J. S.; Lee, S. *Nature* **1995**, *374*, 792.

(11) (a) Tsukube, H.; Shinoda, S. *Chem. Rev.* **2002**, *102*, 2389. (b) Cheetham, A. K.; Ferey, G.; Loiseau, T. *Angew. Chem., Int. Ed.* **1999**, *38*, 3268.

(12) Lwamoto, M.; Furukawa, H.; Mine, Y.; Uemura, F.; Mikuriya, S. I.; Kagawa, S. *J. Chem. Soc., Chem. Commun.* **1986**, 1272.

(13) Piguet, C. *Chimia* **1996**, *50*, 144.

(14) Koeller, S.; Bernardinelli, G.; Bocquet, B.; Piguet, C. *Chem. Eur. J.* **2003**, *9*, 1062.

(15) Kepert, D. *Inorganic Stereochemistry*; Springer: Berlin, 1982; Chapters 2 and 12−16.

(16) Bünzli, J. C. G. *Basic and Applied Aspects of Rare Earths*; Editional Complutense: Madrid, 1997.

(17) (a) Zhao, B.; Cheng, P.; Dai, Y.; Cheng, C.; Liao, D. Z.; Yan, S. P.; Jiang, Z. H.; Wang, G. L. *Angew. Chem., Int. Ed.* **2003**, *42*, 934. (b) Zhao, B.; Cheng, P.; Chen, X. Y.; Cheng, C.; Shi, W.; Liao, D. Z.; Yan, S. P.; Jiang, Z. H. *J. Am. Chem. Soc.* **2004**, *126*, 3012. (c) Goodgame, D. M. L.; Hill, S. P. W.; Williams, D. J. *J. Chem. Soc., Chem. Commun.* **1993**, 1019.

(18) (a) Pan, L.; Huang, X. Y.; Li, J.; Wu, Y. G.; Zheng, N. W. *Angew. Chem., Int. Ed.* **2000**, *39*, 527. (b) Pan, L.; Adams, K. M.; Hernandez, H. E.; Wang, X. T.; Zheng, C.; Hattori, Y.; Kaneko, K. *J. Am. Chem. Soc.* **2003**, *125*, 3062. (c) Dalgarno, S. J.; Raston, C. L. *Chem. Commun.* **2002**, 2216. (d) Gheorghe, R.; Andruh, M.; Mller, A.; Schmidtmann, M. *Inorg. Chem.* **2002**, *41*, 5314. (e) Vaidhyanathan, R.; Natarajan, S.; Rao, C. N. R. *Inorg. Chem.* **2002**, *41*, 4496. (f) Goodgame, D. M. L.; Grachvogel, D. A.; White, A. J. P.; Williams, D. J. *Inorg. Chem.* **2001**, *40*, 6180.

(19) (a) Yaghi, O. M.; O'Keeffe, M.; Ockwig, N. W.; Chae, H. K.; Eddaoudi, M.; Kim, J. *Nature* **2003**, *423*, 705. (b) Eddaoudi, M.; Moler, D. B.; Li, H.; Chen, B.; Reineke, T. M.; O'Keeffe, M.; Yaghi, O. M. *Acc. Chem. Res.* **2001**, *34*, 319.

(20) Wachhold, M.; Kasthuri. R. K.; Lei, M.; Thorpe, M. F.; Billinge, S, J. L.; Petkov, V. *J. Solid State Chem.* **2000**, *152*, 3.

(21) Albertsson, J. *Acta Chem. Scand.* **1970**, *24*, 1213.

(22) Albertsson, J. *Acta Chem. Scand.* **1972**, *26*, 985.

(23) (a) Albertsson, J. *Acta Chem. Scand.* **1972**, *26*, 1005. (b) Albertsson, J. *Acta Chem. Scand.* **1972**, *26*, 1023.

(24) (a) Harrowfield, J. M.; Kim, Y.; Skelton, B. W.; White, A. H. *Aust. J. Chem.* **1995**, *48*, 807. (b) Swarnabala, G.; Rajasekharan, M. V. *Inorg. Chem.* **1998**, *37*, 1483.

(25) Ghosh, S. K.; Bharadwaj, P. K. *Inorg. Chem.* **2003**, *42*, 8250.

Table 1. Crystallographic Data and Structure Refinement for **2**−**5**

	2	**3**	**4**	**5**
empirical formula	$C_{35}H_{47}N_5O_{36}Pr_3$	$C_{21}H_{17}N_3O_{16}Pr_2$	$C_7H_{11}ClNO_{12}Pr$	$C_{14}H_{20}N_2O_{19}Pr_2S$
fw	1536.51	849.20	477.53	834.20
cryst syst	monoclinic	monoclinic	cubic	orthorhombic
space group	*C*2/*c*	*P*2(1)/*c*	*Pa*-3	*Pna*2(1)
a (Å)	22.3971(6)	11.009(3)	20.506(4)	18.800(7)
b (Å)	13.90130(10)	17.546(5)		6.540(2)
c (Å)	17.8650(5)	13.489(4)		18.684(7)
β (deg)	114.4870(10)	101.022(4)		
V (Å^3)	5061.9(2)	2557.8(13)	8623(3)	2297.3(14)
Z	4	4	24	4
F(000)	3028	1640	5568	1616
ρ [Mg/m^3]	2.016	2.205	2.207	2.412
abs coeff (mm^{-1})	2.955	3.852	3.639	4.381
data/restraints/param	4443/0/339	4516/0/379	2553/61/267	3578/1/344
GOF	1.162	1.040	1.094	1.082
R1 ($I = 2\sigma(I)$)[a]	0.0784	0.0245	0.0215	0.0264
wR2 (all data)[a]	0.1779	0.0639	0.0485	0.0590

[a] $R1 = \sum||F_o| - |F_c||/|F_o|$, $wR2 = [\sum w(F_o^2 - F_c^2)^2/\sum w(F_o^2)^2]^{1/2}$.

g), with 45% yield based on Pr, were collected after washing with water and ether. Anal. Calcd for **2**: C, 27.33; H, 3.05; N, 4.56. Found: C, 27.06; H, 2.91; N, 4.39.

{[Pr$_2$(PDA)$_3$(H$_2$O)$_3$]·H$_2$O}$_n$ (3). A mixture of pyridine-2,6-dicarboxylic acid (0.8 mmol, 0.134 g), Pr_6O_{11} (0.1 mmol, 0.102 g), H_2O (10 mL), and C_2H_5OH (2 mL) was placed in a 25 mL acid-digestion bomb at 180 °C for 3 days. The products (0.074 g), with 29% yield based on Pr, were collected after washing with water and ether. Anal. Calcd for **3**: C, 29.39; H, 2.25; N, 4.81. Found: C, 29.67; H, 2.00; N, 4.95.

{[Pr(PDA)(H$_2$O)$_4$]·ClO$_4$}$_n$ (4). A mixture of pyridine-2,6-dicarboxylic acid (0.6 mmol, 0.100 g), 12 mL of H_2O, 2 mL of C_2H_5OH, $HClO_4$ (1.0 mmol), and Pr_6O_{11} (0.1 mmol, 0.102 g) was placed in a 25 mL acid-digestion bomb at 180 °C for 3 days. The products (0.132 g), with 46% yield based on Pr, were collected after washing with H_2O. Anal. Calcd for **4**: C, 17.60; H, 2.32; N, 2.93. Found: C, 17.37; H, 2.42; N, 2.88.

{[Pr$_2$(PDA)$_2$(H$_2$O)$_5$SO$_4$]·2H$_2$O}$_n$ (5). A mixture of pyridine-2,6-dicarboxylic acid (1.2 mmol, 0.200 g), Pr_6O_{11} (0.1 mmol, 0.102 g), $(NH_4)_2SO_4$ (0.6 mmol, 0.080 g), H_2O (12 mL), and C_2H_5OH (2 mL) was conducted into a 25 mL acid-digestion bomb at 180 °C for 3 days. The products (0.085 g) were obtained in a yield of 34% (based on Pr) after washing with H_2O. Anal. Calcd for **5**: C, 20.05; H, 2.67; N, 3.17. Found: C, 20.14; H, 2.40; N, 3.36.

Crystal Structure Determination. Diffraction intensities for complexes **2**−**5** were collected at 293 K on a computer-controlled Bruker SMART 1000 CCD diffractometer equipped with graphite-monochromated Mo Kα radiation with a radiation wavelength of 0.710 73 Å using the *ω*-scan technique. Lorentz polarization and absorption corrections were applied. The structures were solved by direct methods and refined with the full-matrix least-squares technique using the SHELXS-97 and SHELXL-97 programs.[26] Anisotropic thermal parameters were assigned to all non-hydrogen atoms. The hydrogen atoms were set in calculated positions and refined as riding atoms with a common fixed isotropic thermal parameter. Analytical expressions of neutral-atom scattering factors were employed, and anomalous dispersion corrections were incorporated. The crystallographic data and selected bond lengths for **2**−**5** are listed in Tables 1−5. CCDC176385 (**1**), 211242 (**2**), 185546 (**3**), 176384 (**4**), and 219628 (**5**) contain the supplementary crystallographic data for this paper. These data can be obtained free of charge via www.ccdc.can.ac.uk/conts/retrieving.html (or from the Cambridge Crystallographic Centre, 12 Union Road, Cambridge CB21EZ, UK; Fax: (+44) 1223−336033; or deposit@ccdc.cam.ac.uk).

(26) (a) Sheldrick, G. M. *SHELXS 97, Program for the Solution of Crystal Structures*; University of Göttingen: Göttingen, Germany, 1997. (b) Sheldrick, G. M. *SHELXL 97, Program for the Refinement of Crystal Structures*; University of Göttingen: Göttingen, Germany, 1997.

Table 2. Selected Bond Lengths (Å) for **2**[a]

Pr1−O9	2.508(9)	Pr1−O3	2.482(10)	Pr2−O4#2	2.455(9)
Pr1−O1#1	2.535(9)	Pr1−O9#1	2.508(9)	Pr2−O11	2.585(11)
Pr1−N3	2.575(16)	Pr2−O7	2.444(10)	Pr2−O13	2.612(12)
Pr1−N1	2.610(12)	Pr2−O10	2.460(10)	Pr2−O14	2.540(11)
Pr2−O5	2.450(10)	Pr2−O12	2.649(11)	Pr2−N2	2.593(11)

[a] Symmetry transformations used to generate equivalent atoms: #1 $-x + 1, y, -z + 1/2$; #2 $-x + 3/2, y + 1/2, -z + 1/2$; #3 $-x + 3/2, y - 1/2, -z + 1/2$.

Table 3. Selected Bond Lengths (Å) for **3**[a]

Pr(1)−O(9)	2.466(3)	Pr(1)−O(2)#1	2.468(3)
Pr(1)−O(6)	2.495(3)	Pr(1)−O(4)#1	2.546(3)
Pr(1)−O(7)	2.564(3)	Pr(1)−O(7)#2	2.580(3)
Pr(1)−O(15)	2.598(3)	Pr(1)−N(1)#1	2.607(3)
Pr(1)−N(2)	2.640(3)	Pr(2)−O(12)#3	2.353(3)
Pr(2)−O(5)	2.371(3)	Pr(2)−O(3)	2.394(3)
Pr(2)−O(11)#4	2.484(3)	Pr(2)−O(13)	2.510(3)
Pr(2)−O(10)#4	2.533(3)	Pr(2)−O(14)	2.579(3)
Pr(2)−N(3)#4	2.595(3)		

[a] Symmetry transformations used to generate equivalent atoms: #1 $x + 1, y, z$; #2 $-x + 2, -y, -z + 2$; #3 $-x + 1, y + 1/2, -z + 5/2$; #4 $-x + 1, -y, -z + 2$; #5 $x - 1, y, z$; #6 $-x + 1, y - 1/2, -z + 5/2$.

Table 4. Selected Bond Lengths (Å) for **4**[a]

Pr1−O4	2.473(3)	Pr1−O3#1	2.527(3)	Pr1−O7	2.530(3)
Pr1−O2	2.475(3)	Pr1−O5	2.524(3)	Pr1−O8	2.527(3)
Pr1−O6	2.483(3)	Pr1−N1	2.619(3)	Pr1−O1#2	2.537(3)

[a] Symmetry transformations used to generate equivalent atoms: #1 $y + 1/2, z, -x + 1/2$; #2 $y, -z + 1/2, x - 1/2$; #3 $z + 1/2, x, -y + 1/2$; #4 $-z + 1/2, x - 1/2, y$.

Results and Discussion

Crystal Structure of {[Pr(PDA)(HPDA)(H$_2$O)$_2$]·4H$_2$O}$_n$ (1). Complex **1** was synthesized and characterized by X-ray diffraction analysis independently in our lab, which was also reported by Ghosh et al. recently.[25] The structure of **1** consists of linear chains of Pr(III) ions, and each metal ion shows a coordination number of nine, binding two PDA ligands, one bridging carboxylate O atom, and two water molecules. In

Table 5. Selected Bond Lengths (Å) for **5**[a]

Pr(1)−O(16)	2.469(5)	Pr(1)−O(15)	2.483(5)
Pr(1)−O(14)	2.489(5)	Pr(1)−O(17)	2.523(5)
Pr(1)−O(13)	2.518(5)	Pr(2)−O(3)	2.431(6)
Pr(1)−O(7)	2.547(5)	Pr(1)−O(1)	2.640(5)
Pr(2)−O(10)#2	2.609(5)	Pr(2)−O(7)	2.497(5)
Pr(2)−O(5)	2.539(5)	Pr(2)−N(1)	2.637(7)
Pr(2)−O(11)	2.616(5)	Pr(2)−O(1)	2.624(5)
Pr(2)−N(2)	2.679(6)	O(6)−Pr(1)#4	2.520(5)
Pr(2)−O(9)	2.654(5)	O(12)−Pr(2)#3	2.719(4)
Pr(1)−O(6)#1	2.520(5)		

[a] Symmetry transformations used to generate equivalent atoms: #1 $x - 1/2, -y + 3/2, z$; #2 $x, y + 1, z$; #3 $x, y - 1, z$; #4 $x + 1/2, -y + 3/2, z$.

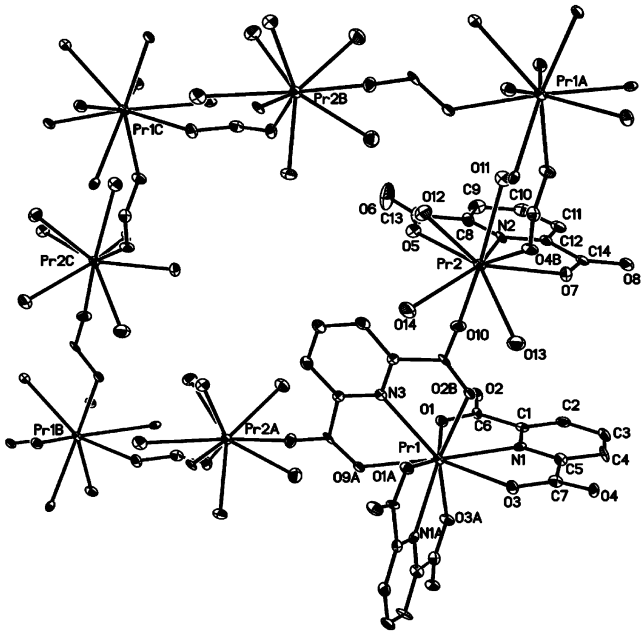

Figure 1. Nanosized square motif containing eight Pr ions and coordination environment of the Pr ion in complex **2**.

this work we introduced **1** for two reasons: (a) To illustrate a successful investigation by simply tuning different Pr/PDA ratios to obtain different complexes from a 1D chain to 3D network; (b) To design and synthesize **5** based on the motif of **1**.

Crystal Structure of $\{[Pr_3(PDA)_4(HPDA)(H_2O)_8]\cdot 8H_2O\}_n$ (2). The single-crystal analysis of **2** reveals that Pr atoms have two types of coordination environments (Figure 1), and all Pr atoms show a coordination number of nine with a tricapped trigonal prism geometry. Pr1 atom chelates to three PDA molecules: six oxygen atoms and three nitrogen atoms form coordination sphere of the Pr1 atom. The average dihedral angle between the three PDA pyridine rings is 90.6°, while the Pr2 atom only chelates to one PDA molecule: four oxygen atoms from the carboxylate groups of PDA ligand, four water molecules, and one nitrogen atom of PDA ligand (Pr2−N2 = 2.593(11) Å) complete the coordination geometry of the Pr2 atom. The distance between Pr1 and Pr2 atoms is 6.990(9) Å. A similar coordination geometry has been observed in other PDA−Ln systems.[26]

Two Pr atoms with different coordination modes are alternately arrayed by carboxylate bridges and generated a nanosized octanuclear homometallic Pr_8 square unit with a

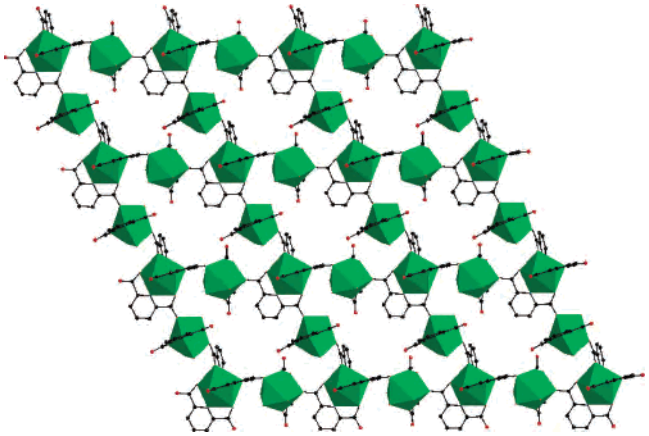

Figure 2. Diamond view of 2D grid motif assembled by square unit as the building block in **2**: Green, Pr; red, O; black, C; black line, bond.

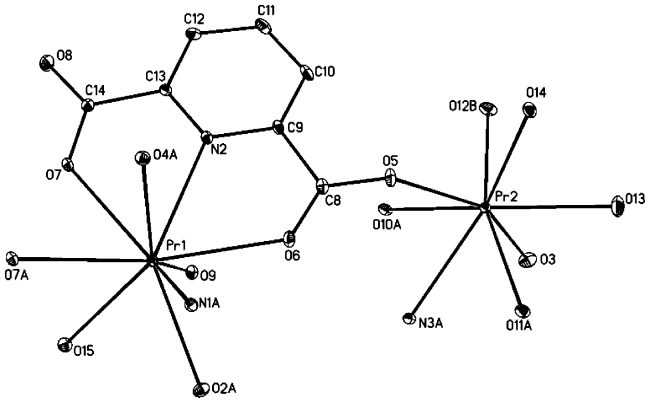

Figure 3. Structure of dinuclear Pr unit in **3** showing the coordination environment of the Pr center. Uncoordinated water molecules and H atoms were omitted for clarity.

32-membered $Pr_8C_8O_{16}$ motif, the Pr atoms possessing three PDA anions located on the vertex of a square, while the Pr atoms possess one PDA anion occupied in the middle of each edge with an identical length of 13.180(10) Å. The eight Pr atoms are almost coplanar with a mean deviation from the plane of 0.2012 Å. Most importantly, the square structure as a building block is further assembled into a spectacular 2D grid (Figure 2). To our knowledge, **2** is the first example to exhibit a highly ordered 2D grid assembled through the Pr_8 square unit in lanthanide-based complex, although many such highly ordered motifs containing transition metals have been documented.[27] Various hydrogen bonds exist between the carboxylate oxygen and solvent water or coordinated water molecules (see Supporting Information); as a result, the 2D grids are further assembled by hydrogen bonds to form a 3D supramolecular network. These hydrogen bonds help stabilize the unusual topologies of **2**.

Crystal Structure of $\{[Pr_2(PDA)_3(H_2O)_3]\cdot H_2O\}_n$ (3). The single-crystal analysis of **3** reveals that Pr atoms exhibit two types of coordination environments (Figure 3), namely, nine-coordinate Pr1 and eight-coordinate Pr2. The Pr1 atom

(27) (a) Cabarrecq, C. B.; Fernandes, A.; Jaud, J.; Costes, J. P. *Inorg. Chim. Acta* **2002**, *332*, 54. (b) Ciurtin, D. M.; Smith, M. D.; zur Loye, H.-C. *Chem. Commun.* **2002**, 74. (c) Daiguebonne, C.; Guillou, O.; Kahn, M. L.; Kahn, O.; Oushoorn, R. L.; Boubekeur, K. *Inorg. Chem.* **2001**, *40*, 176.

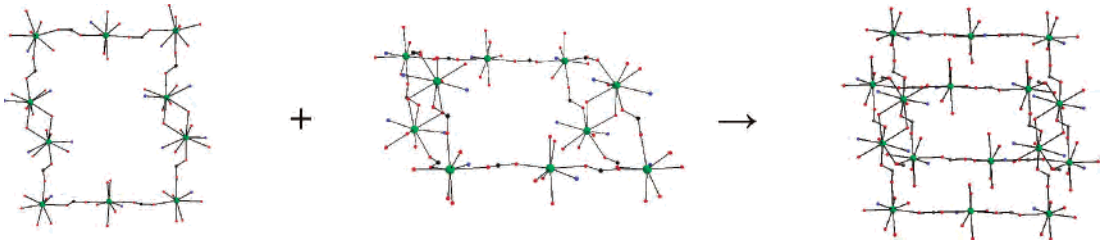

Figure 4. Grids interpenetrate of two types Pr_{10} metallic macrocycles in **3**: C, black; N, blue; O, red; Pr, green.

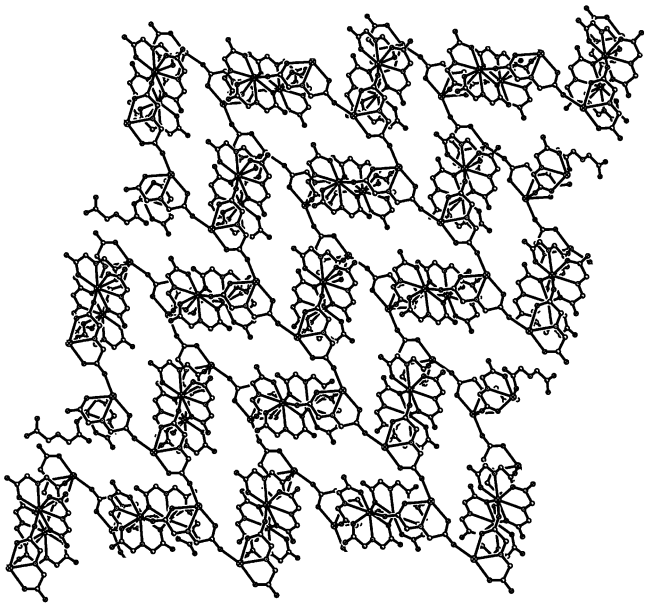

Figure 5. 2D square-grid network architecture of **3** assembled by the Pr_{10} ring as a building block along the *c* direction. Hydrogen atoms and some carbon atoms of the PDA ligands have been omitted for clarity.

coordinates to two oxygen atoms from the carboxylate group, two chelated tridentate PDA molecules, and one water molecule: seven oxygen atoms and two nitrogen atoms (Pr1−N1A 2.607(3) Å, Pr1−N2 2.640(3) Å) form the tricapped trigonal prism configuration of Pr1 atom. The Pr2 atom only chelates to one PDA molecule: three oxygen atoms from the carboxylate group of PDA ligand, four water molecules, and one nitrogen atom of the PDA ligand complete coordination geometry of the Pr2 atom. These Pr−O and Pr−N bond lengths are slightly shorter than those in the La−PDA complex,[26] as expected due to lanthanide contraction. The distance between the Pr1 and Pr2 atoms is 6.554(3) Å. Two Pr atoms with a different coordination mode are alternately arrayed by carboxylate bridges to generate a decanuclear homometallic Pr_{10} square unit with a 38-membered $Pr_{10}C_8O_{20}$ motif (Figure 4). The 10 Pr atoms are almost coplanar with a mean deviation from the plane of 0.259 Å. Most importantly, viewed along the [001] direction, the square structure as a building block is further assembled into a spectacular and ordered 2D network (Figure 5). These decanuclear homometallic units also interpenetrate to form a 3D polymer, as shown in Figure 6.

Crystal Structure of $\{[Pr(PDA)(H_2O)_4]\cdot ClO_4\}_n$ (4). The hexanuclear praseodymium ring structure in **4** is shown in Figure 7; each Pr atom chelates to one PDA molecule; eight oxygen atoms and one nitrogen atom (Pr1−N1 = 2.619(3) Å) complete the coordination sphere of the Pr atom, which conforms most closely to a tricapped trigonal prism. Adjacent Pr atoms are linked by the carboxylate group of the PDA ligand, which results in construction of the hexanuclear Pr ring with an ideal C_3 symmetry. 6Pr, 6C, and 12O atoms form a 24-membered ring, which was further considered as a subunit and mutually connected through carboxylate bridges to assemble into a 3D framework (Figure 8). The distance between neighboring Pr atoms is 6.284(3) Å, and the separation of the opposing Pr···Pr is 11.583(6) Å in the ring. Remarkably, only a few examples of lanthanide ring-like structures have been reported to date: tetranuclear La and Nd,[28] hexanuclear Sm[29] and Eu,[30] octanuclear La,[31a] and decanuclear Dy[31b] ring. However, these reported rings only exhibit isolated molecular structures rather than assembling further into multidimensional structure through utilizing the ring as a building block. Though Rao reported two 3D Nd complexes containing 12-membered channels previously,[32] complex **4** is a rather rare 3D polymer constructed by the building blocks of large rare-earth rings. It is noted that ClO_4^- anions exist as guests in the pores of 3D network hosts (Figure 9). The cavity of the network is about 0.43 nm, which may be a potential microporous materials for gas adsorption.

Crystal Structure of $\{[Pr_2(PDA)_2(H_2O)_5SO_4]\cdot 2H_2O\}_n$ (5). The molecular structure of **5** is shown in Figure 10, exhibiting a binuclear praseodymium entity connected by carboxylic oxygen bridges. The coordination numbers of Pr1 and Pr2 are 8 and 10, respectively. Unchelated PDA ligand on Pr1 ion was observed, and only five water molecules and three carboxylic oxygen atoms complete the coordination sphere of the Pr1 atom. The average Pr−O bond length of 2.524 Å is slightly longer than the reported value previously.[33] While the Pr2 atom shows a 10-coordinate environment, two PDA act as a tridentate ligand (ONO) chelated to Pr2 occupying six coordination sites of the Pr2 atom. Two sulfate anions as bidentate ligands (OSO) fulfill the remaining

(28) (a) Barnhart, D. M.; Clark, D. L.; Gordon, J. C.; Huffman, J. C.; Watkin, J. G.; Zwick, B. D. *J. Am. Chem. Soc.* **1993**, *115*, 8461. (b) Obora, Y.; Ohta, T.; Stern, C. L.; Mark, T. J. *J. Am. Chem. Soc.* **1997**, *119*, 3745.
(29) (a) Anwander, R. *Angew. Chem., Int. Ed.* **1998**, *37*, 599. (b) Ganesan, M.; Gambarotta, S.; Yap, G. P. A. *Angew. Chem., Int. Ed.* **2001**, *40*, 766.
(30) Yann, B.; Marinella, M.; Jacques, P.; Mariyn, M. O. *J. Am. Chem. Soc.* **2002**, *124*, 9012.
(31) (a) Xu, J.; Raymond, K. N. *Angew. Chem., Int. Ed.* **2000**, *39*, 2745. (b) Westin, L. G.; Kritikos, M.; Caneschi, A. *Chem. Commun.* **2003**, 1012.
(32) Vaidhyanathan, R.; Natarajan, S.; Rao, C. N. R. *Inorg. Chem.* **2002**, *41*, 4496.
(33) Martin, L. L.; Jacobson, R. A. *Inorg. Chem.* **1972**, 2789.

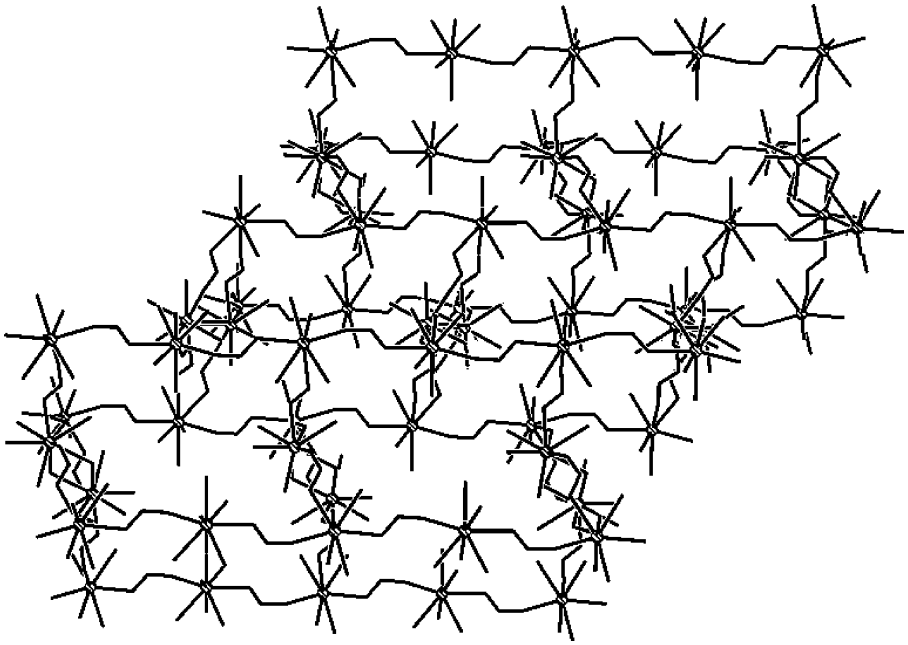

Figure 6. 3D coordination network of **3** constructed via Pr_{10} metallic macrocycles interpenetration. Only carboxylic ones in all carbon atoms were retained for clarity.

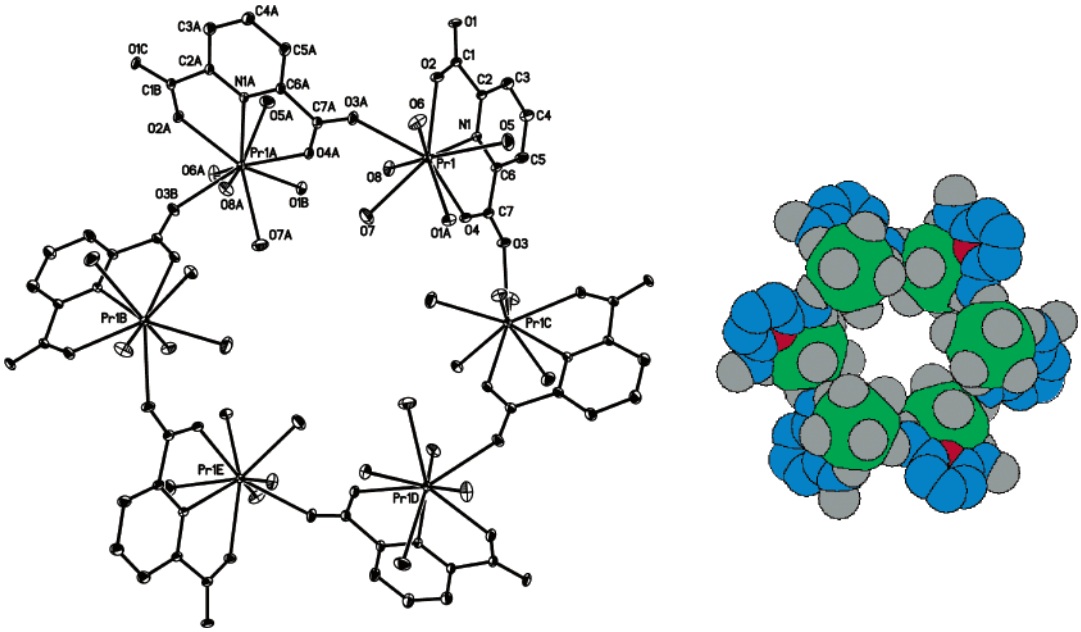

Figure 7. Hexanuclear Pr metallic macrocycle motif with ideal C_3 symmetry and coordination sphere of Pr ions in complex **4** (left). Space-filling representation down the C_3 axis of the hexanuclear Pr ring structure as building blocks in **4** (right): C, blue; N, red; O, gray; Pr, green.

four coordination sites. The separations of Pr2−S1A and Pr2−S1 are 3.2665(18) and 3.2756(18) Å, respectively, which are slightly longer than 3.056(7) Å of the reported Pr−S bond.[34] We may consider that interactions exist between Pr and S atoms, and sulfate anions may be seen as tridentate ligands since the sum of the van der Waals radii of Pr and S is slightly longer than 3.4 Å. It must be noted that there is only one crystallographically independent SO_4^{2-} anion in the molecular motif, although two sulfate anions chelated to a Pr center. The dihedral angle between pyridine rings connected to the Pr2 atom is 28.4°, with a small deviation from the coplanar case. Actually, from the stereochemical effect point of view, without coordination of SO_4^{2-} anions, the closer the dihedral angle is to 90°, the more stable the configuration of **5**. Obviously, the SO_4^{2-} anions chelated to the Pr2 atom from both upper and down directions result in the formation of such a small dihedral angle. Two sets of oxygen atoms of sulfate anion, (O9, O11) and (O10, O12), and the S1 atom form two planes with a dihedral angle of 90.3°, and the bond lengths of S−O are nearly equal, varying from 1.470 to 1.493 Å. All angles of O−S−O in a sulfate ion slightly deviate from those of an ideal tetrahedron, which is sufficient to reduce the local environment from T_d to C_{2v} for the S atom.

(34) Pinkerton, A. A.; Schwarzenbach, D. *J. Chem. Soc., Dalton Trans.* **1976**, 2464.

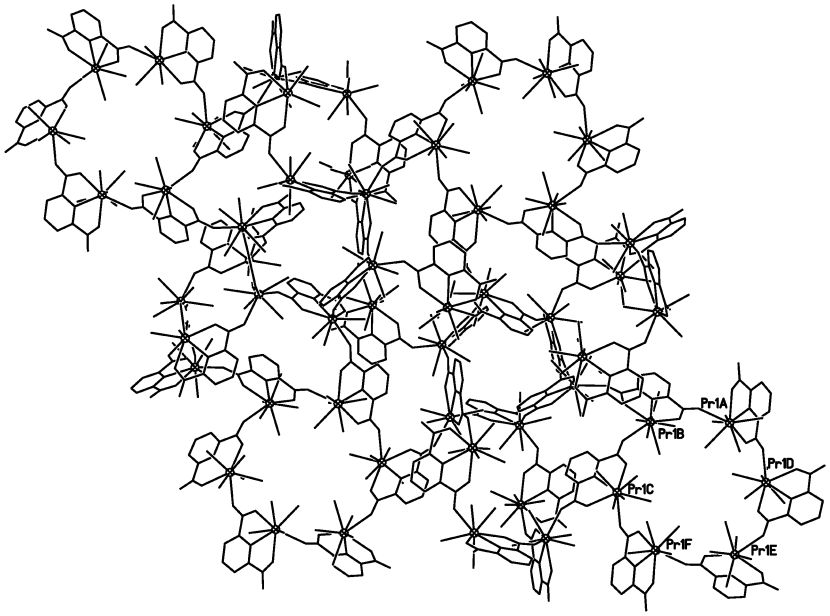

Figure 8. 3D network of **4** assembled by the hexanuclear Pr ring as a building block.

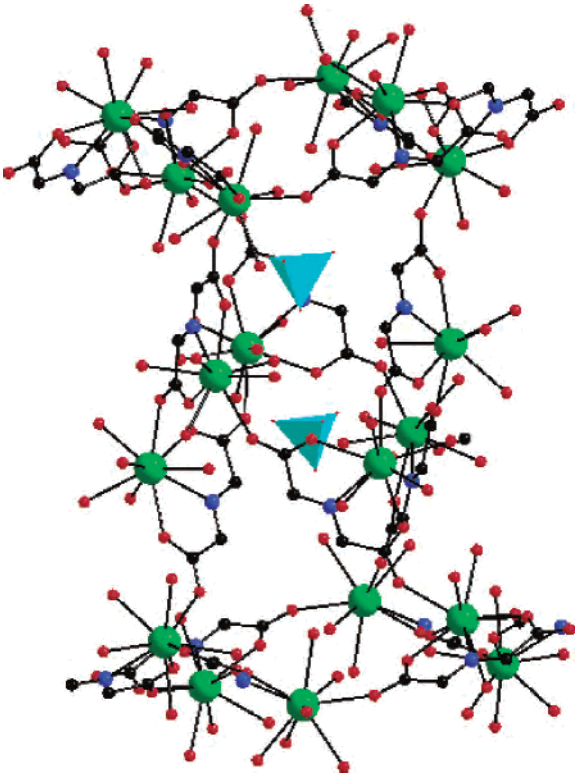

Figure 9. ClO_4^- as guests existing in the host network of **4**: cyan diamond, ClO_4^-; green, Pr; red, O; blue, N; black, C.

Two Pr atoms with different coordination modes are alternately arrayed by carboxylate bridges to generate a 1D chain motif along the *a* axis, and the SO_4^{2-} anions further connect the 1D chain to construct an unusual 2D grid through a unique bi-bidentate chelated mode along the *b* axis (Figure 11). The repeat unit in the 2D grid exhibits a rectangular configuration consisting of six Pr atoms with a size of 6.540 × 9.514 Å^2. The possible coordination modes of the sulfate ligand in the complexes exhibit considerable diversity, as

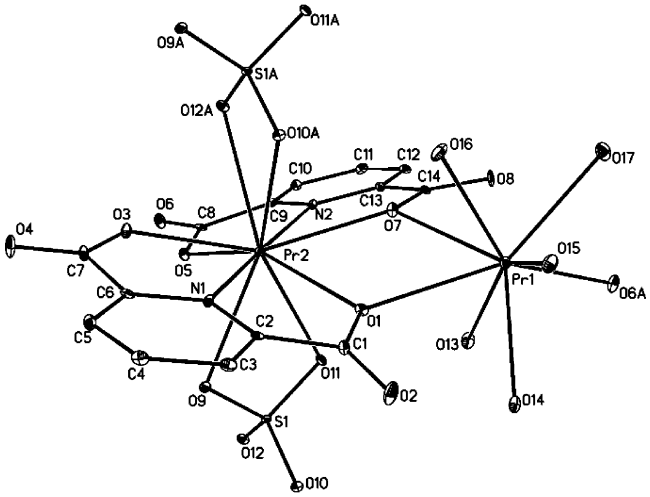

Figure 10. Structure of the dinuclear Pr unit in **5** showing the coordination environment of the Pr center. Solvent water and H atoms were omitted for clarity.

shown in Scheme 1, and among them the mode **D** has not been reported hitherto. To the best of our knowledge, this is a rather rare 2D lanthanide-based grid constructed by bi-bidentate SO_4^{2-} anions. Uncoordinated water molecules link the 2D grids through hydrogen bonding to form a 3D supramolecule (Supporting Information). In addition, the pyridine rings of PDA ligands between adjacent 2D layers parallel and partly overlap with a distance of ca. 3.4 Å, generating relatively strong $\pi-\pi$ interactions. Compared with the 2D compound **2**, both hydrogen bonds and $\pi-\pi$ interactions help stabilize the 2D grid structure of **5**.

Pr/L Ratio and Structure. In summary, by tuning different Pr/PDA ratios slightly under the same synthesis conditions, we obtained complexes **1**−**3** successfully, which exhibit dramatically different topological structures from a 1D chain, to a 2D grid, to a 3D network. The relationships between the Pr/PDA ratio and the structures are listed in

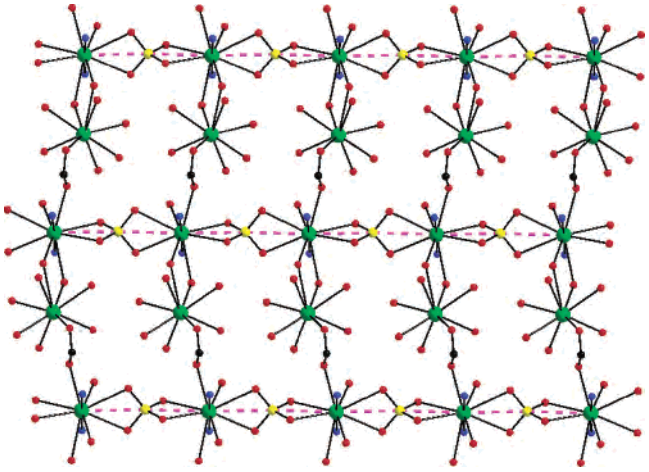

Figure 11. 2D grid motif of **5** exhibiting the repeat unit structure consisting of six Pr atoms and the bi-bidentate coordinated mode of SO_4^{2-} anion: green, Pr; red, O; green, N; yellow, S; black, C; black line, coordinated or covalent bond; purple dot, Pr−S weak interaction.

Scheme 1 Possible Coordination Modes of the Sulfate Anion

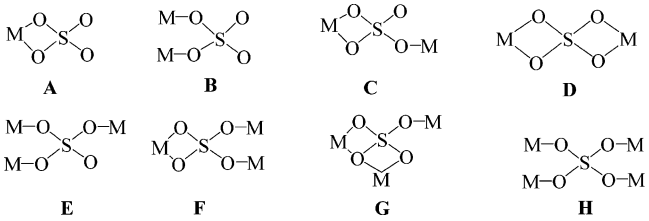

Table 6. Though Pr atoms have different coordination spheres, we find that a subtle change of the Pr/PDA ratio is the predominant factor resulting in significant differences in structural dimensionalities. In Table 6 **1** is a 1D chain with a Pr/PDA ratio of 1/2 in the synthesis while **2** is a 2D grid with a Pr/PDA ratio of 3/5, which is slightly larger than the Pr/PDA ratio of **1**. It is noticeable that while the synthetic ratio of Pr/PDA is 3/4 and 1/1, 3D polymers **3** and **4** can be obtained in the synthetic system, respectively. The case exhibits that enlarging the M/L ratio may be a method to achieve 3D coordination polymers. On the other hand, anions in the synthetic systems may be another important factor for forming the multidimensional structures. The perchlorate anions occupy the cavities in **4,** while SO_4^{2-} anions in **5** coordinate to the metal centers and enhance the dimensionality from a 1D chain to a 2D grid. This work may be a successful example enriching the field of Ln-based complexes in controlling self-assembly as well as devotion to the subjects of crystal design and engineering.

Self-Assembled Synthesis of 5 from 1. Actually the synthetic strategy employed for **5** was triggered and further performed only after complex **1** was structurally characterized (Scheme 2). Taking into account that the coordination number of Pr could vary from 8 to 12[35a] and two water molecules coordinated to Pr^{3+} in **1**, we wondered whether **1** could be transformed into a more interesting and higher dimensional structure by replacing the coordinated water molecules located on the Pr ion by anionic species. Using hydrothermal synthesis and introducing sulfate anions into the reagent system of complex **1**, the expected complex-like motif **A** was not obtained (shown in Scheme 2) and unexpectedly a highly ordered 2D grid complex **5** (motif **B**) was formed. Compared with **1**, coordinated water molecules were replaced by sulfate anions to have the coordination environment of Pr2 in **5** as anticipated; therefore, the 1D chainlike structure of **1** was transformed into the 2D grid motif of **5** by introduction of the sulfate bridges.

TGA and PXRD. Thermal gravimetric analyses (TGA) of **2** show three regions of weight loss. From room temperature to 120 °C uncoordinated water molecules were lost. Complete loss of water is achieved only above 420 °C, which shows that the water molecules are tightly held to the metal ion. TGA results of **3** show that uncoordinated and coordinated water molecules were lost together between 80 and 220 °C, and further weight loss took place at about 300 °C. Compared with the TGA of **2**, the results of **5** show similar temperature regions of weight loss. Uncoordinated water molecules were lost from room temperature to 125 °C, and coordinated ones were removed below 410 °C. Complete decomposition is achieved only above 450 °C in each case. Powder X-ray diffraction (PXRD) of compounds **2**−**5** has been studied at room temperature. The patterns calculated from the single-crystal structures described hereafter **2**−**5** are in good agreement with the observed ones (Figure 12 and Supporting Information), which confirms that the single-crystal structures are really representative of the bulk of the corresponding samples.

FT-IR Spectra. Since complexes **2**−**5** have the same PDA ligand and Pr centers, we just exampled the FT-IR results of **5**. In the FT-IR spectra the strongly absorbing bands at 1680 and 1377 cm^{-1} can be assigned to vibration of $\nu_{as}(CO_2^-)$ and $\nu_s(CO_2^-)$, respectively.[35b] The FT-IR results also support the lower local environment, C_{2v}, of S in SO_4^{2-} anion. Three bands were expected for both υ_3 and υ_4 vibrations.[7a] Three bands appearing at 607, 657, and 697 cm^{-1} are particularly evident for υ_4, and three bands at higher wavenumbers (1078, 1095, and 1127 cm^{-1}) could be related to υ_3. While the band observed at 971 cm^{-1} is the υ_1 mode of SO_4^{2-}, the one at 1016 cm^{-1} may be assigned to either υ_1 or υ_3.

Magnetic Properties. It is well known that for systems containing Ln ions the effects of the magnetic exchange coupling are much weaker than those of transition-metal ions because the f orbitals are well shielded by outer s and p orbitals and less extended than d orbitals of transition-metal ions. In addition, analysis of the magnetic interaction between rare-earth ions, except Gd(III), gives rise to additional difficulties since the magnitude of these interactions is comparable with that of the crystal field acting on the ion due to the large orbital contribution. As a result, isolation of the single-ion magnetic anisotropy from the exchange contribution in the analysis of the temperature dependence of the magnetic susceptibility is a largely unachieved task. As far as Pr^{3+} is concerned, it possesses rather large

(35) (a) Drew, M. G. B. *Coord. Chem. Rev.* **1977**, *24*, 179. (b) Yang, L.; la Cour, A.; Anderson, O. P.; Crans, D. C. *Inorg. Chem.* **2002**, *41*, 6322.

Table 6. Investigation of Pr/PDA Ratio and Anions in the Syntheses and Structures

	molecular structure	Pr/PDA(synthesis)	Pr/PDA(structure)	dimensionality	anions(synthesis)
1	$\{[Pr(PDA)(HPDA)(H_2O)_2]\cdot 4H_2O\}_n$	3/6	0.500	one	
2	$\{[Pr_3(PDA)_4(HPDA)(H_2O)_8]\cdot 8H_2O\}_n$	3/5	0.600	two	
3	$\{[Pr_2(PDA)_3(H_2O)_3]\cdot H_2O\}_n$	3/4	0.667	three	
4	$\{[Pr(PDA)(H_2O)_4]\cdot ClO_4\}_n$	3/3	1.000	three	perchlorate
5	$\{[Pr_2(PDA)_2(H_2O)_5SO_4]\cdot 2H_2O\}_n$	2/1	1.000	two	sulfate

Scheme 2. 1D Structure of **1** Transformed into a 2D Grid of **5** by Introduction of Sulfate Anions under Hydrothermal Condition[a]

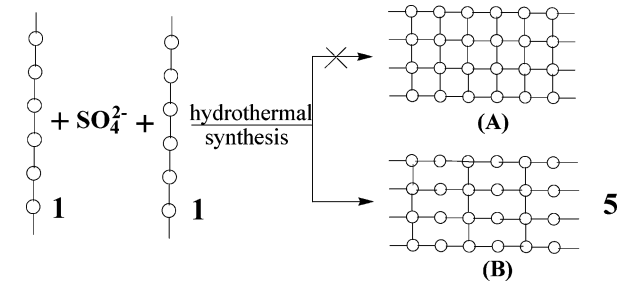

[a] ○ represents Pr atoms.

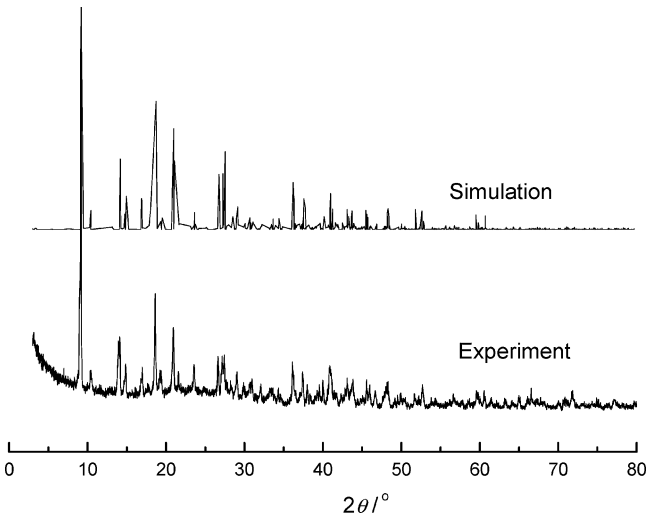

Figure 12. PXRD for complexes **5** (as a representative example).

unquenched orbital angular momentum associated with the internal nature of the valence f orbitals and simultaneously has orbitally degenerate ground states, which are facile to be split by spin−orbit coupling and crystal-field effects. The magnetic properties of Pr(III) ions are strongly influenced by the factors mentioned above.

The magnetic susceptibilities of **2**, **4,** and **5** were measured in the temperature range from 5 to 300 K as shown in Figure 13. The $\chi_M T$ values are equal to 4.72, 1.51, and 3.15 cm^3 K mol^{-1} at room temperature, respectively, which are slightly lower than those expected (4.81 (**2**), 1.60 (**4**), and 3.20 (**5**) cm^3 K mol^{-1}) per insulated Pr ion in the $^3H_4$ ground state (g = 4/5). Although the $\chi_M T$ values for **2**, **4,** and **5** smoothly decrease with decreasing temperature, antiferromagnetic coupling between adjacent Pr ions could not be explicitly deduced due to the existence of strong spin−orbit coupling for lanthanide atoms. The decrease in $\chi_M T$ possibly originates in the thermal depopulation of the highest Stark components deriving from the splitting of the free-ion ground state $^3H_4$ by the crystal field.[36] Accordingly, any weak exchange interaction within the structure is masked by crystal-field effects, and no conclusions can therefore be drawn about its value and sign for these products.

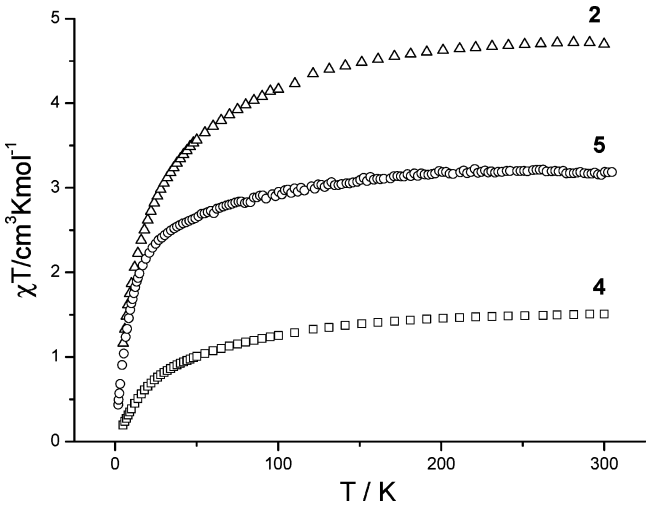

Figure 13. Plots of $\chi_M T$ vs T for **2**(△), **4**(□), and **5**(○).

Conclusion

The title complexes exhibit completely different topological structures. **2** displayed a novel 2D grid assembled by an octanuclear Pr square unit as a building block and is, to our knowledge, reported for the first time to fabricate 2D polymers through such high-regular lanthanide units. Complex **3** exhibited a decanuclear homometallic Pr_{10} square structure with a 38-membered $Pr_{10}C_8O_{20}$ motif, which can interpenetrate to form a 3D coordination polymer, while in **4** the 24-membered ring with six Pr ions as a building block was further assembled into a very rare 3D complex in lanthanide coordination chemistry. **5** is an interesting 2D Pr-based polymer, which was designed and synthesized after **1** was structurally characterized under hydrothermal conditions. Importantly, the repeat unit in the grid consisted of six Pr ions, two SO_4^{2-} anions, and four carboxylic oxygen bridges, exhibiting an intriguing rectangular configuration. Most remarkably, although the rich coordination modes of SO_4^{2-} anions were well documented, its bi-bidentate coordination mode has been rarely observed so far, and hopefully this work fills the gap.

A successful synthetic strategy by tuning the Pr/PDA ratio (from 1/2, 3/5, to 3/4) to control the structures was applied under the same reaction conditions (hydrothermal synthesis). As a result, a series of high-dimensional coordination polymers **1**−**3** was isolated with a Pr/PDA ratio from 1/2, 3/5, to 2/3 in the structures. To our knowledge, systematic investigation of the lanthanide complexes with a different

(36) Costes, J. P.; Clemente-Juan, J. M.; Dahan, F.; Nicodème, F.; Verelst, M. *Angew. Chem., Int. Ed.* **2002**, *41*, 323.

Ln/L ratio in a synthesis system has been not carried out before this work. Noticeably, some anions such as ClO_4^- and SO_4^{2-} may play a key role in constructing polymers. The ClO_4^- anions in **4** were trapped in the cavity and may stabilize the 3D framework of **4**, whereas SO_4^{2-} anions in **5** were directly associated with forming the 2D grid.

This work not only expands the field of known lanthanide coordination polymers, but also is expected to instigate great progress in self-assembly networks of lanthanide complexes. On the basis of this work, further synthesis and structural studies for other lanthanide coordination polymers with different Ln/L ratios are underway in our lab.

Acknowledgment. This work was supported by the National Natural Science Foundation of China (Nos. 90101028 and 50173011) and the TRAPOYT of MOE China.

Supporting Information Available: Additional synthetic details and figures and crystallographic data in CIF format. This material is available free of charge via the Internet at http//pubs.acs.org.

IC049498M